Vol. 48, No. 3 (2026) 577-594, DOI: 10.24874/ti.2259.06.26.08

Tribology in Industry

www.tribology.rs

RESEARCH

Assessment of Two Body Abrasive Wear Performance of PA66 Composites Under Multi-Pass Conditions Using Taguchi-GRA-PCA Optimization

S.M. Vinu Kumar[a,*], E. Sakthivelmurugan[b], A.T. Ravichandran[c], J.P. Rishi[d], B. Harshavardhan[e], P. Balamurugan[f]

[a]*Department of Mechanical Engineering, Sri Krishna College of Engineering and Technology, Kuniyamuthur, Coimbatore, Tamil Nadu, India,*
[b]*Department of Mechanical Engineering, Bannari Amman Institute of Technology, Sathyamangalam, TN, India,*
[c]*Department of Mechanical Engineering, Vel Tech Rangarajan Dr. Sagunthala R&D Institute of Science and Technology, Chennai, Tamil Nadu, India,*
[d]*Department of Mechanical Engineering, Vidyavardhaka College of Engineering, Mysuru, Karnataka, India,*
[e]*Department of Mechanical Engineering, The National Institute of Engineering, Mysuru, Karnataka, India,*
[f]*Department of Mechanical Engineering, Kalasalingam Academy of Research and Education, Krishnankoil, TN, India.*

Keywords:

Abrasive wear
PA66 composites
Short glass fiber
Multi-response optimizatio
Principal component analysis

* Corresponding author:

S.M. Vinu Kumar
E-mail: vinukmr1988@gmail.com

Received: 15 June 2026
Revised: 17 July 2026
Accepted: 10 August 2026

A B S T R A C T

This study systematically explores the two-body abrasive wear (2BAW) performance of neat Polyamides66 (PA66), short glass fiber reinforced PA66 (PA66/SGF) and talc filled short glass fiber reinforced hybrid composites (PA66/SGF/T). 2BAW test was performed using pin on disc machine as per ASTM G99 for different operating conditions against silicon carbide water proof emery paper. Experimental layouts were designed based on the Taguchi's L_9 orthogonal arrays for the input parameters such as sliding distance (75, 100, and 125 m), applied load (5, 10, and 15 N) and reinforcement type (PA66, PA66/SGF, and PA66/SGF/T). Grey relational analysis (GRA) and principal component analysis (PCA) were integrated with Taguchi to analyze the effect of input factors on the multiple responses namely, coefficient of friction (COF), specific wear rate (SWR) and hardness of the composites. Analysis of variance (ANOVA) was employed to identify the significant factors affects the abrasive wear characteristics of the PA66 composites. The results indicated that addition of SGF and talc fillers into the PA66 matrix increased the wear resistance. Higher wear resistance to the 2BAW under multipass condition was exhibited by the PA66/SGF/T hybrid composites. Worn surfaces of the PA66 composite specimens were examined using field emission scanning electron microscopy (FESEM) photographs. The observations revealed that transition of wear mechanism from mild to severe wear with increasing sliding distance and applied load, mainly characterized by ploughing, matrix tearing, shallow grooves and fiber breakages. Taguchi-GRA-PCA method suggested that 2BAW performance of the PA66 composite was mainly contributed by sliding distance followed by reinforcement type and applied load

1. INTRODUCTION

Thermoplastic polymers have taken a special place in engineering applications owing to their superior combination of mechanical, physical, and anti-corrosion properties along with favorable tribological behaviour and ease of fabrication. Therefore, thermoplastics are employed in making tribo-components such as bushes, bearings, cams, rollers, and bearing cages typically interacting with ceramic, metallic and polymer counterparts [1]. Polyamides are one such famous thermoplastics made of amide bonds, known as cast nylons. PA6 and PA66 plastics garnered a momentous interest to use in advance engineering applications but not limited to construction, automotive and aerospace industries due to their exceptional durability with high tensile strength and light weight properties. However, polyamides are susceptible to water absorption due to the presence of amino groups [2,3].

In an industrial application it is inevitable for the engineering components to slide against each other and eventually results in friction and wear problems. However, most of the wear problems are mainly due to the abrasive wear, which accounts for 60% of the total cost [4,5]. In abrasive wear, hard material slides against the soft material under the application of load during which surface asperities of harder material eventually removes the softer material [5]. Worn soft materials are no longer perform its function as required due to severe damages endured and thus needed replacement to prevent the catastrophic failure. However, expenses of the replacement are certain and can be controlled by reducing the intensity of the abrasive wear to a maximum extent [6]. This is can be accomplished by either using higher wear resistant material or reinforced polymer composites and also by optimizing testing conditions. Glass fibers, carbon fibers, talc, wood flour and glass beads are widely used as reinforcing materials in thermoplastic composites and supports in enhancing loading bearing and wear resistance of the composites [7,8]. Savaş et al. [9] reported that incorporation of basalt fiber enhanced the hardness and abrasive wear performance of the high-density polyethylene composites. Tong et al. [10] found that increasing the aspect ratio of fiber was crucial in improving the abrasive wear resistance of the wollastonite fiber reinforced ultra-high molecular weight polyethylene composites. Tribological properties of the polyaryletherketone composites were studied by Harsha et al. [11]. They reported that specific wear rate (SWR) of two body abrasive wear was 5-12 times higher than three body abrasion wear. Several researchers reported that polymer blending was considered as an effective way of improving the mechanical and wear properties in the field of polymer tribology. Moreover, studies showed that tribological performance of the blended composites were par with the neat polymer component [12]. Zhou et al. [13] observed that addition of carbon fiber into the blends of polyamide6/polyphenylene sulfide composites enhanced the wear of the composites. They also found the wear mechanism was primarily adhesive wear. Lingesh et al. [14] demonstrated that addition of micro-fillers in polyamide 66 and polypropylene (PA66/PP) blends have improved the two-body abrasive wear behaviour of the composites. Moreover, operating conditions such as sliding distance, and abrasive grain size influenced abrasive wear resistance of the composites. Lucas et al. [15] revealed that incorporation of UHMWPE to the HDPE enhanced the abrasion wear resistance of the blended composites. Reinforcements of the graphite and nanoclay with the blends of polyamide66/polypropylene (PA66/PP) was studied by Kumar et al. [16]. They revealed that addition of particulates had improved the wear resistance of the composite under varying abrading distance. Mimaroglu et al. [17] established that higher surface roughness of the worn surface implies higher wear rate as reported for the PA6 composites reinforced with glass beads, talc, and wollastonite fillers. Kumar et al. [18] explored the two-body abrasive wear performance of the Nylon6 and glass fiber reinforced Nylon6 composites. They reported that addition of 30wt.% of glass fibers helps in improving the wear resistance of the Nylon6 composites. SWR decreases with increase in the fiber content. However, reinforcing SGF with polyurethane (PU) increases the wear volume of the composites as studied by Suresha et al.

[19]. Hybridization of short carbon fiber and PTFE particulate in PA66 exhibited better wear resistance. Load and particle size of the abrasives were the important factors affected the wear performance of the PA66 composites as reported by Tewari et al. [20]. Implementation of optimization tools for the tribological studies not only reduces the experimental cost but also assists in identifying the optimal parameters responsible for minimum wear and friction. Several studies have reported the successful application of statistical methods for determining the key parameters affecting the performance characteristics including the Taguchi technique [21-25], Grey relational analysis [26-29] and Taguchi-GRA integrated PCA [30-32].

Hybridization of glass fibers and talc filler with polymer matrix have demonstrated the balanced combination of mechanical strength, stiffness and tribological performances compared to the single reinforcements [33-35]. In our previous report, erosion wear performance of the PA66 composites reinforced with glass fibers and talc was methodically investigated and confirmed the significant effect of process parameters on the erosion wear rate and erosion efficiency of the PA66 composites. The study also showed transition in wear behaviour from ductile to semi-ductile in both neat PA66 and PA66 hybrid composites [34]. However, erosion wear differs significantly from the two-body abrasion wear, where direct surface to surface contact governs the wear mechanism. Furthermore, only few studies have been reported on the two-body abrasive wear behavior of PA66 hybrid composites under controlled sliding condition. Therefore, present study has been undertaken to study the effect of short glass fibers and talc fillers on two body abrasive wear behaviour of PA66 composites using silicon carbide abrasive paper using Taguchi-GRA-PCA method. Furthermore, this study mainly focused to gain the global understanding of the wear parameters such sliding distance, applied load and reinforcement type. Outcome of the study expected to promote the practical implementation of the PA66 composites in tribological applications.

2. MATERIALS AND METHODS

2.1 Materials used

PA66 granules were procured from Grand pacific petrochemical corporation, Taiwan. Short glass fibers (SGFs) with fiber length of 3mm and aspect ratio in the range 100-500, were used as a primary reinforcement member and supplied by Nippon Electric Glass -Malaysia. Talc particles with a size of size 3-8µm and an aspect ratio 10-30, were employed to serve as a secondary reinforcement member for the fabrication of PA66 hybrid composites. Fig. 1 presents the surface morphology and elemental composition of talc filler.

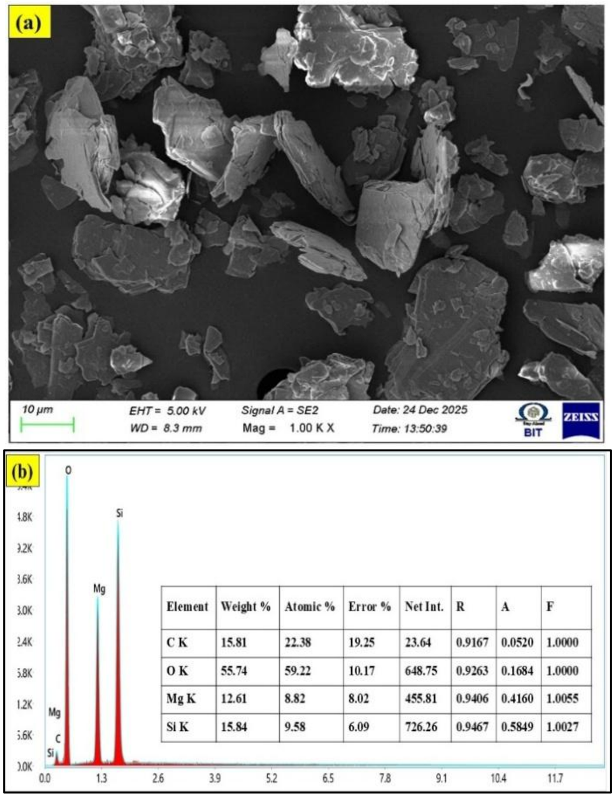

Fig. 1. (a) FESEM micrograph of the talc filler (b) EDS spectrum of the talc filler confirming major elements [34].

2.2 Fabrication of the PA66 composites

PA66 granules, SGFs, and talc fillers were initially dried using hot air oven at the temperature range 95-105 °C for 3 hours to remove the moisture content. These dried constituents were weighted as per the requirement and pre-mixed in a mechanical grinder to ensure uniform distribution of the constituents. Subsequently homogenous mixture was fed into the twin-screw extrusion machine for the achieving the melt compounding. The extrusion process was performed at the controlled temperature conditions, with the hopper throat maintained between 70-90 °C. The barrel temperature profile for the different zones is shown in the Fig. 2. Screw speed in the range 80 to 120 rpm was used for the uniform dispersion of the reinforcements with in the matrix phase. Extrudates were eventually cooled using a water bath and then pulled through the mechanical puller and pelletizing into granules by means of mechanical cutter. To ensure the smooth processing, these granules were dried at 95-105 °C before subjecting to injection moulding process. Finally, dried PA66/SGF/T composite granules were injection moulded in to the required specimen dimensions with the mould temperature between 55-95 °C. Fabricated specimens were conditioned at toom temperature before using them for testing. The compositions of the composites with their designation are presented in Table 1.

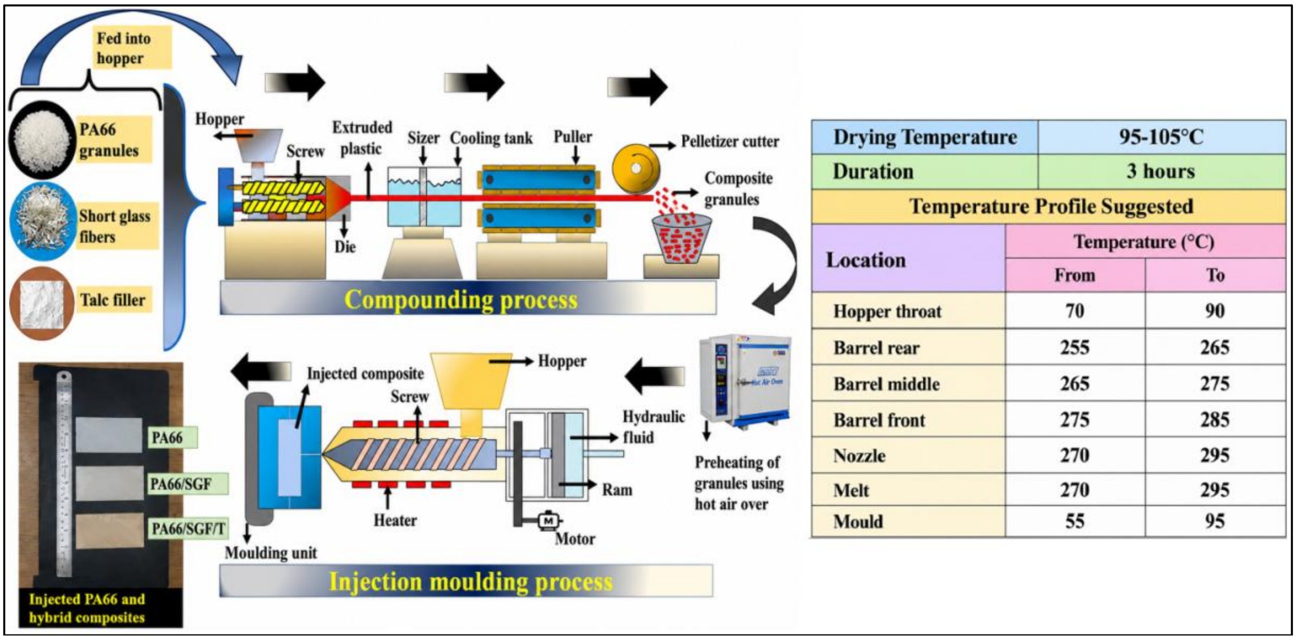

Fig. 2. Steps followed for preparing of the PA66 based composites.

Table 1. Composition of the various PA66 composites.

Material	Designation	PA66 (wt.%)	Short glass fiber (SGF) (wt.%)	Talc filler (wt.%)	Density (g/cc)
Neat PA66	PA66	100	-	-	1.136
PA66 reinforced with SGF	PA66/SGF	60	40	-	1.510
Talc filled PA66/SGF	PA66/SGF/T	52	40	8	1.521

2.3 Two body abrasive wear (2BAW) test of PA66 composites

Pin on disc tribometer was employed to explore the two body abrasive wear properties of the PA66 composite specimens as per ASTM G99 [4]. The 2BAW test was performed at room temperature where composite specimen with dimension 3 mm ×3 mm ×3 mm prepared and firmly attached to the stainless-steel pin of 6 mm diameter as shown in the Fig. 3. Before the testing, contact surface of the PA66 composite specimen was polished using emery papers to ensure uniform surface then specimens were brought into contact with the rotating disc covered with abrasive paper. The disc was rotated at pre-determined speed to reach the required sliding velocity. For each test, four trials were conducted and fresh abrasive paper was used for every trail. The key factors such as sliding distance, applied load, and reinforcement type were varied according to the experimental design. While testing, frictional force was continuously monitored to determine the coefficient of friction (COF). After the test, worn specimens were cleaned using acetone to remove any debris and weighed using high precision electronic balance with an accuracy ±0.1 mg to determine the mass loss.

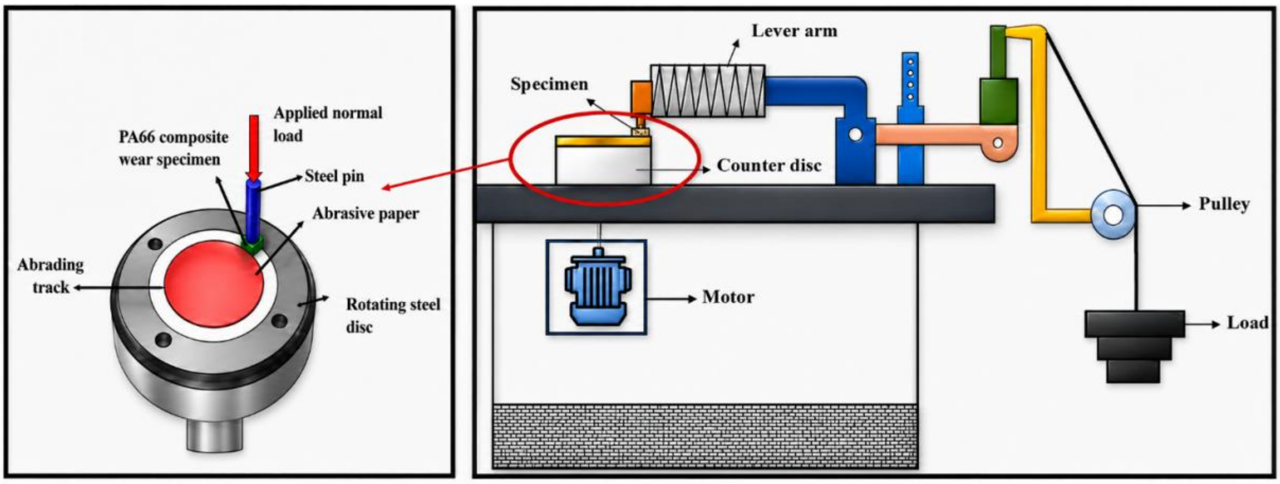

Fig. 3. Experimental setup of two body abrasive wear test.

COF, wear rate and SWR were calculated using equations (1), (2), and (3), respectively.

$$COF = \frac{\text{Frictional force}\,(F_f)}{\text{Normal load}\,(N_L)} \quad (1)$$

$$\text{Wear rate} = \frac{\Delta m}{\rho D_s}\ (mm^3/m) \quad (2)$$

$$SWR = \frac{\Delta m}{\rho F_f D_s}\ (mm^3/N-m) \quad (3)$$

Where, Δm - Weight loss of the specimen (g), ρ - Density of the composite (g/cc), F_f - Frictional force (N), N_L- Applied normal load (N), and D_s - Sliding distance (m).

Worn out PA66 composite samples along with the worn abrasive paper is presented in the Fig. 4.

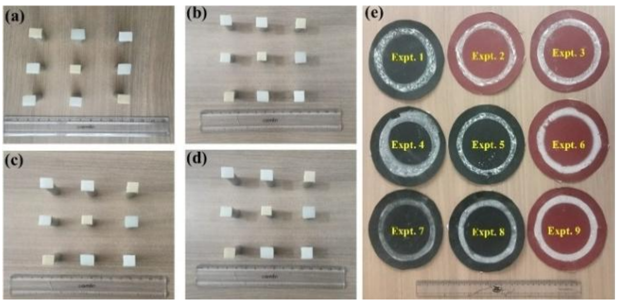

Fig. 4. (a-d) Worn samples of PA66 composites under multipass condition (e) Abraded emery papers.

2.4 Taguchi Design of Experiment

Genichi Taguchi developed DOE technique with robust experimental designs mainly intended to reduce set of experimental trials based on orthogonal arrays (OAs). In this investigation, input factors and their levels considered for 2BAW under multi-pass conditions is shown in the Table 2. L_9 OA was chosen as per the T-DOE methodology to design the experimental trials as generated from MINITAB 16 software. Experimental layout of the 2BAW study of PA66 composites for the different input combination with corresponding output responses is detailed in the Table 3.

Many researchers have successfully implemented various statistical tools to optimize the wear performance of the composites. However, the Taguchi method remains as widely adopted approach owing to its simplicity and effectiveness, particularly employed for solving the single objective optimization problem with reduced number of trials, thereby saves time and resources without compromising in providing sufficient information which eventually facilitates in analysing the system. Optimization of the abrasive wear performance of PA66 composites using T-DOE follows systematic and structured procedure, starting with the data collection, progress through analysis and interpretation. First step in T-DOE begins with transforming the experimental data into signal to noise (S/N) ratios, which further act as a measure of performance variability. These S/N ratios are classified as higher the better (HB), lower the better (LB) and nominal the better (NB) based on the desired characteristics of the output response.

Table 2. Control factors and their levels for 2BAW of PA66 composites.

Control factors	Symbol	Units	Levels		
			1	2	3
Sliding distance	A	m	75	100	125
Applied load	B	N	5	10	15
Reinforcement type	C	wt.%	PA66	PA66/SGF	PA66/SGF/T
Constant factors: sliding velocity-0.5 m/s, track diameter-100 mm, SiC based water proof emery paper-320 grit size					

Table 3. Experimental design for 2BAW using L_9 OA along with its output response characteristics.

Experiment No.	Sliding distance (m)	Applied load (N)	Reinforcement type	Response Characteristics		
				SWR (mm3/N-m)	COF	Shore-D hardness
1	75	5	PA66	0.02653±0.00175	0.020±0.00423	84±0.750
2	75	10	PA66/SGF	0.03794±0.00246	0.030±0.00674	85±1.125
3	75	15	PA66/SGF/T	0.02671±0.00361	0.033±0.00616	89±1.450
4	100	5	PA66/SGF	0.02833±0.00318	0.020±0.00348	85±1.125
5	100	10	PA66/SGF/T	0.02110±0.00152	0.100±0.00451	89±1.450
6	100	15	PA66	0.02893±0.00271	0.087±0.00689	84±0.750
7	125	5	PA66/SGF/T	0.05018±0.00399	0.160±0.00725	89±1.450
8	125	10	PA66	0.03092±0.00438	0.070±0.00987	84±0.750
9	125	15	PA66/SGF	0.03710±0.00506	0.100±0.00368	85±1.125

In the present study, responses such SWR, and COF are classified under the LB criterion, as minimizing these values are very crucial for enhancing the wear performance of the PA66 composites whereas for the response hardness is categorized under HB criterion, as hardness of the composite improves wear resistance property. These criteria are evaluated using equations (4-6). The responses are transformed to S/N ratios by means of logarithmic function as described in equations (7-9), mainly facilitates for the effective optimization and in-depth analysis.

$$L_{HB} = \frac{1}{X}\sum_{i=1}^{n}\frac{1}{R_{hrd}^{2}} \quad (4)$$

$$L_{LB} = \frac{1}{X}\sum_{i=1}^{n}\frac{1}{R_{SWR}^{2}} \quad (5)$$

$$L_{LB} = \frac{1}{X}\sum_{i=1}^{n}\frac{1}{R_{COF}^{2}} \quad (6)$$

Where, R_{hrd}^2, R_{swr}^2 and R_{COF}^2 represents the response for hardness, specific wear rate and coefficient of friction, 'X' denotes number of experiments.

$$\text{S/N ratio for shore-D hardness} = -10\log_{10}(L_{HB}) \quad (7)$$

$$\text{S/N ratio for SWR} = -10\log_{10}(L_{LB}) \quad (8)$$

$$\text{S/N ratio for COF} = -10\log_{10}(L_{LB}) \quad (9)$$

2.5 Grey relational analysis (GRA)

GRA developed by Deng Julong (1982) and considered as an effective technique for addressing the multi-response optimization problems. Initially experimental data are normalized between 0 to 1 value through a process called grey relational generation which specifically eliminates the dimensional inconsistencies. In the next steps, Grey Relational Coefficient (GRC) is determined from the normalized data to establish the relationship among ideal and experimental results. In the GRA approach, each experimental trail comprising of multiple response parameter is converted into single performance index termed as Grey Relational Grade (GRG). The GRG is evaluated by taking the average of GRC values corresponding to all response characteristics.

Thus, converting the multi-response optimization problem into single objective.

Furthermore, Analysis of Variance (ANOVA) is applied for the GRG values to identify the impact of the input factors on the abrasive wear performance of the PA66 composites. The following steps are followed to determine GRG:

(i) Normalization of SWR and COF data follows LB criterion as determined by using equation (10)

$$Y_i(z) = \frac{\max Q_i(z) - Q_i(z)}{\max Q_i(z) - \min Q_i(z)} \quad (10)$$

HRD (Shore D hardness) follows higher the better criterion, as expressed in equation (11)

$$Y_i(z) = \frac{Q_i(z) - \min Q_i(z)}{\max Q_i(z) - \min Q_i(z)} \quad (11)$$

Where Qi(z) is the obtained value, min $Q_i(z)$ is the minimum value for the z^{th} response and max $Q_i(z)$ is the maximum value for the k^{th} response.

(ii) Deviation sequence is determined using equation (12).

$$\Delta_{oi} = \left| Q_o(z) - Q_i(z) \right| \quad (12)$$

Where, Qo (z) and Qi (z) is reference and comparability sequence respectively. Δ0i is the deviation sequence of the aforesaid sequences.

(iii) GRC is calculated using equation (13)

$$\zeta(z) = \frac{\Delta_{\min} + \beta\Delta_{\max}}{\Delta_{oi}(z) + \beta\Delta_{\max}} \quad (13)$$

Where β is the identification coefficient value, considered as 0.5 when equal weightage is given to the input process parameters.

(iv) Final steps involve calculation of GRG using an equation (14).

$$\psi_i(GRG) = \frac{1}{n_r}\sum_{z=1}^{n} \zeta_i(z) \quad (14)$$

(v) PCA is employed to assign the weight values to an individual response and GRG is determined by using formula (15). In the GRA integrated PCA approach, each GRC is multiplied by its respective weight before summation to arrive GRG. Generally, GRG values between 0 to 1, with higher values implies better correlation between input parameters and performance characteristics. Therefore, higher GRG represents better optimal parametric combinations.

$$\psi_i(GRG) = \sum_{z=1}^{n} \omega_z \zeta_i(z) \quad (15)$$

Where, ψ_i denotes GRG for the i^{th} experiment and n represent the number of the response characteristic. During practical application, influence of each control factors is not same in the output characteristics. Therefore, equation (14) is modified to expression (15), where 'ω_z' indicates the weighted value of the z^{th} response evaluated from PCA.

2.6 Principal component analysis (PCA)

Principal Component Analysis (PCA), a multivariate statistical tool first proposed by Pearson in 1901 and later modified by Hotelling in 1933. In this investigation, PCA has been employed to evaluate the weightage contribution of each response characteristics associated with 2BAW performance of PA66 composites under multipass condition.

The following steps are followed in PCA:

(i) To construct the variance and co-variance matrix 'Ci' using equation (16).

$$C_i = \begin{bmatrix} C_1(1) & C_1(2) & . & . & C_1(n) \\ C_2(1) & C_2(2) & . & . & C_2(n) \\ . & . & . & . & . \\ . & . & . & . & . \\ C_e(1) & C_e(2) & . & . & C_e(n) \end{bmatrix} \quad (16)$$

Where, 'e' denotes number of the experimental run, 'n' represents number of the response characteristics. 'C' indicates the GRC of an individual performance characteristic. For the present studies on abrasion wear, e=9, and n = 3.

(ii) Computation of correlation coefficient arrays using equation (17).

$$V_{xL} = \left(\frac{\mathrm{cov}(C_i(x), C_i(L))}{\sigma_{ci}(x) \times \sigma_{ci}(L)} \right) \quad (17)$$

Where cov ($C_i(x)$, $C_i(L)$) are covariance of the sequence $C_i(x)$, and $C_i(L)$ respectively. $\sigma C_i(x)$ and $\sigma C_i(L)$ denotes the S.D of the sequence $C_i(x)$, and $C_i(L)$ respectively.

(iii) Evaluation of Eigen values and Eigen vectors using the correlation coefficient arrays using equation (18)

$$(V - \lambda_k I_e) P_{ik} = 0 \tag{18}$$

Where λ_k denotes the Eigen values; $\sum_{k=1}^{n} \lambda_k = n$, where k=1, 2, 3, ………..n.

P_{ik} represents, $P_{ik} = [a_{k1}, a_{k2}, a_{k3}, \ldots \ldots .. a_{ke}]^T$ Eigen vectors corresponding to Eigen values λk.

(iv) In the final step, principal components are computed using equation (19)

$$E_{mk} = \sum_{i}^{n} C_e(i) \times P_{ik} \tag{19}$$

Where, E_{e1} represents as first component, E_{e2} as second principal components and so on. Confirmation test was performed to validate the experimental results.

2.7 Shore D hardness

Shore-D hardness tester was used for finding the Shore-D hardness of the PA66 composite samples according to ASTM D2240 [36]. A minimum of five trials were conducted, and the average of their readings was calculated as the hardness of the PA66 composites.

2.8 FESEM

The worn morphology of the PA66 composite samples and abrasive emery paper was explored by using FESEM technique (Make: Carl Zeiss Sigma-300, Schottky FEG) under different magnifications.

3. RESULT AND DISCUSSION

In the present investigation, the experimental parameters such as reinforcement type, applied load, and sliding distance are varied while the sliding velocity, track diameter, and abrasive paper grit size are kept constant. The testing conditions and its parameter levels for evaluating the 2BAW behaviour of PA66 composites is presented in the Table 2. Specific wear rate (SWR), coefficient of friction (COF) and hardness of the composites are considered as output responses. The main objective of this study is to minimize the SWR and COF while maximizing the hardness of the PA66 composites. Based on the Taguchi's design techniques, L_9 OA is employed to establish the strong relationship between the process parameters and the responses. Accordingly, the experimental results of the 2BAW responses namely SWR, COF and hardness of the PA66 composites are presented in the Table 3.

Initially, the output responses are normalized using equations (10) and (11) following estimation of the deviation sequences corresponding to the normalized data using equation (12). Subsequently, the grey relational coefficient (GRC) values are computed from the deviation sequence data using equation (13). The normalized values, deviation sequences and GRC data for the PA66 composites are detailed in the Table 4. The eigenvalues and the percentage of variation determined by the principal component analysis for 2BAW test of PA66 composites is shown in Table 5.

Table 4. Normalized, Deviation and GRC Data for 2BAW Test of PA66 composites.

Exp. No	Normalized Value			Deviation Sequence			Grey Relational Coefficient (GRC)		
	Specific Wear rate	COF	Shore-D hardness	Specific Wear rate	COF	Shore-D hardness	Specific Wear rate	COF	Shore-D hardness
1	0.8135	1.0000	0.0000	0.1865	0.0000	1.0000	0.7284	1.0000	0.3333
2	0.4212	0.9286	0.2000	0.5788	0.0714	0.8000	0.4635	0.8750	0.3846
3	0.8073	0.9048	1.0000	0.1927	0.0952	0.0000	0.7218	0.8400	1.0000
4	0.7517	1.0000	0.2000	0.2483	0.0000	0.8000	0.6682	1.0000	0.3846
5	0.9998	0.4286	1.0000	0.0002	0.5714	0.0000	0.9997	0.4667	1.0000
6	0.7309	0.5238	0.0000	0.2691	0.4762	1.0000	0.6501	0.5122	0.3333
7	0.0008	0.0000	1.0000	0.9992	1.0000	0.0000	0.3335	0.3333	1.0000
8	0.6627	0.6429	0.0000	0.3373	0.3571	1.0000	0.5972	0.5833	0.3333
9	0.4503	0.4286	0.2000	0.5497	0.5714	0.8000	0.4763	0.4667	0.3846

Table 5. Eigen value and explained variation for 2BAW test.

Principal component	Eigen value	Explained variation (%)
PC1	1.7622	59.99
PC2	0.588	20.02
PC3	0.587	19.99

In the Taguchi-Grey Relational Analysis (GRA), the weighted values of the output response characteristics are determined using the Principal Component Analysis (PCA) approach. The computed eigenvectors and the contribution of each response characteristics to the 2BAW performance of the PA66 composites are presented in Table 6. The Grey Relational Grade (GRG) values are calculated by incorporating the weighted values of the individual wear performance characteristics using equation (15).

The GRG is the most significant parameter in the statistical analysis, as it transforms multiple response quality characteristics into a single representative index. Based on the obtained GRG values, the experimental runs are ranked in descending order, with the highest GRG value assigned the first rank. Table 7 shows the GRG value and its rank for the 2BAW test of PA66 composites. The first rank is assigned to the third experiment because it exhibits the highest GRG value of 0.2786. This indicates that the response characteristics obtained in the third experiment are the closest to the ideal condition. Based on the GRG results presented in Table 7, the third experimental run exhibits superior overall wear performance by minimizing the specific wear rate and coefficient of friction while maximizing the hardness of the PA66 composites.

Table 6. Eigen Vectors and Contribution of the individual response characteristics for the principal components under 2BAW.

Output response characteristics	Eigen vectors			Contributed/weighted value
	PC1	PC2	PC3	
Specific wear rate	0.679	-0.042	0.733	0.461
COF	0.566	-0.607	-0.558	0.320
Shore-D hardness	0.469	0.794	-0.338	0.220

Table 7. GRG value and its rank for 2BAW of PA66 composites.

Exp. No	Grey relational grade (GRG)	Rank
1	0.2549	2
2	0.2114	5
3	0.2786	1
4	0.2523	3
5	0.2508	4
6	0.1718	7
7	0.1597	8
8	0.1771	6
9	0.1502	9

The effect of the Grey Relational Grade (GRG) on the selected control parameters is shown in Fig. 5. The abrasive wear performance characteristics in terms of GRG for 2BAW test are shown in the Table 8. The optimal combination of input control parameters corresponding to the highest GRG value is identified as A1 (75 m), B1 (5 N), and C3 (PA66/SGF/T). Based on these results, aforementioned combinations are considered as the optimal set of input parameters for achieving the best overall multi-response performance by the PA66 composites under two body abrasive mode. Furthermore, the response Table 8 indicates that sliding distance exhibits the highest GRG value, followed by reinforcement type and applied load. This observation clearly suggests that sliding distance is the most influential parameter affecting the two-body abrasive wear performance of the PA66 composites.

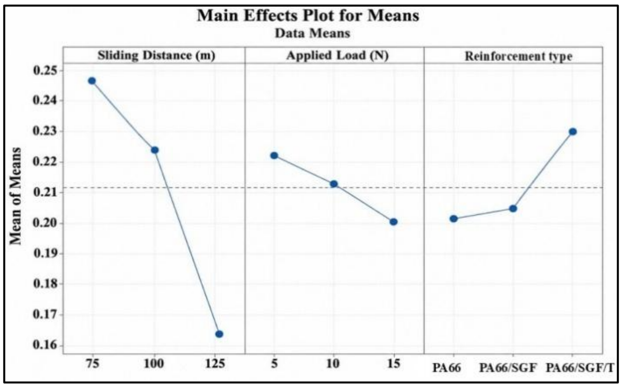

Fig. 5. Effect of input control parameters on multi response characteristics.

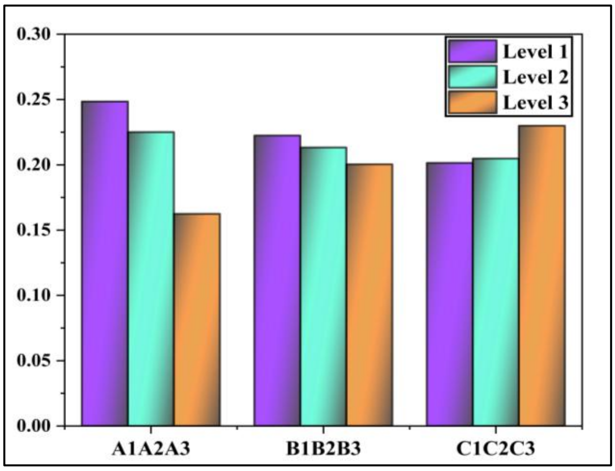

Fig. 6. Graphical representation of GRG.

From the Fig. 6, it is evident that a higher GRG value indicates better wear performance of the composite samples, as it corresponds to lower SWR, lower COF, and higher hardness. The GRG value decreases significantly with an increase in sliding distance from 75 m to 125 m. The reduction in GRG at the higher sliding distance is owing to prolonged abrasive interaction between the composite surface and counterface, which promotes surface fatigue, accumulation of wear debris, and removal of the protective tribo-layer. These mechanisms increase material removal and frictional instability resulting in higher SWR and COF [37,38].

Similarly, the applied load has a significant effect on the GRG value. The GRG decreases with an increase in load from 5 N to 15 N, indicating better wear performance at lower load conditions. At higher loads, increased contact pressure between the composite and counterface leads to plastic deformation of the polymer matrix, damage at the matrix-reinforcement interface, and breakdown of the transfer film. Subsequently, increased wear debris formation and surface degradation results in higher SWR and COF, thereby reducing the overall GRG value [30,39].

Table 8. Response for GRG under 2BAW.

Symbol	Control factors	Grey Relational Grade (GRG)			Main effect (Max-Min)	Rank
		Level-1	Level-2	Level-3		
A	Sliding distance (m)	0.2484	0.2250	0.1624	0.0860	1
B	Applied load (N)	0.2224	0.2132	0.2003	0.0221	3
C	Reinforcement type	0.2014	0.2047	0.2298	0.0289	2

The impact of reinforcement type shows an increasing trend in GRG with an increase in reinforcement level, where hybrid composite PA66/SGF/T exhibits the highest GRG value. This improvement can be attributed to the enhanced hardness, improved load-bearing capacity, and better resistance to abrasive action provided by the hybrid reinforcements [40,41]. The presence of glass fibers and talc filler helps to maintain a stable tribo-layer, which minimizes direct contact between the composite surface and abrasive counterface, thereby reducing wear and friction. Therefore, based on the GRG analysis, the optimal wear performance with minimum SWR and COF was achieved by the hybrid composite PA66/SGF/T when covering sliding distance of 75 m under the application load of 5 N.

3.1. Analysis of variance for 2BAW behaviour of PA66 composites

Analysis of Variance (ANOVA) is employed to identify the most significant contribution of the control parameters toward optimizing the abrasive wear behaviour of the system. The ANOVA for the Grey Relational Grade (GRG) is performed using MINITAB 16 software, and the results are depicted in the Table 9. The analysis reveals that sliding distance is the most influential parameter affecting the abrasive wear behaviour of the PA66 composites, contributing 63.10%, followed by reinforcement type and applied load. Therefore, sliding distance plays a dominant role in governing the abrasive wear performance of the PA66 composites.

Table 9. ANOVA of GRG for dry 2BAW.

Source	DF	Adj SS	Adj MS	F-value	P-value	Contribution (%)
Sliding distance (m)	2	0.011857	0.005928	2.50	0.286	63.10
Applied load (N)	2	0.000741	0.000370	0.16	0.865	03.94
Reinforcement type	2	0.001446	0.000723	0.30	0.766	07.69
Error	2	0.004744	0.002372			25.25
Total	8	0.018788				

Finally, the confirmation test serves as the last step of the statistical analysis. After determining the optimal wear parameters, the experimental results are validated through a confirmation test using the predicted GRG obtained from equation (20).

$$\delta^* = \delta_m + \sum_{i=1}^{n} (\delta_i - \delta_m) \quad (20)$$

Where δ^* is the predicted mean of GRG, δ_m is the total mean of GRG, δ_i is the mean of GRG at optimum level and n is the number of input parameters affecting the multi response characteristics.

The results showed that the experimental GRG value (0.2767) closely agrees with the predicted GRG value (0.3104) with a percentage error of 10.86% as indicated in the Table 10. This deviation may be ascribed to experimental variability, uncontrolled parameters, and model limitations. Furthermore, material heterogeneity and integration effect of GRA-PCA weighting may contribute to the minor differences. Nevertheless, close agreement and consistent trend confirm the satisfactory predictive capability of Taguchi- GRA-PCA approach.

Table 10. GRG confirmation test for 2BAW.

	Predicted –A1B1C3	Experimental-A1B1C3
GRG-value	0.3104	0.2767

3.2. Worn surface morphology of PA66 based composites

2BAW performance of the polymer composites is strongly governed by the evolution of surface morphology worn under varying testing conditions. In the present investigation, abraded surface of the PA66 based composites were observed under varying sliding distances and applied loads. At lower sliding distance (75 m) and applied load (5 N), all PA66 based composites showed relatively mild wear behaviour as it is characterized by smooth and shallow wear tracks, implies minimal material removal. Worn surface of the PA66 exhibits fine micro-ploughing marks and localized adhesive patches which might have occurred owing to the soft nature of matrix material. Under this operating condition (75m and 5N), contact temperature remains low, averting severe softening of matrix and thus wear is restricted to mild plastic deformation [42,43].

In case of PA66/SGF composite, addition of SGFs improves the overall load bearing capacity. Worn surface clearly reveals reduced ploughing and fewer adhesive patches unlike the neat PA66, as presence of glass fibers strongly restricts the matrix deformation [44]. Moreover, from the Fig. 7a evident that fibers have well embedded within the PA66 matrix and minimal fiber exposure is observed.Furthermore, worn surface of the PA66/SGF/T hybrid composite clearly disclosed smoother surface owing to the strong interfacial bonding and synergistic effect of reinforcements. FESEM image (Fig. 7b) shows the thin and continuous transfer film, termed as tribo-film, which eventually act a protective layer against the sliding surface. Further this tribo-film reduces the direct asperity contact and stabilizes friction.

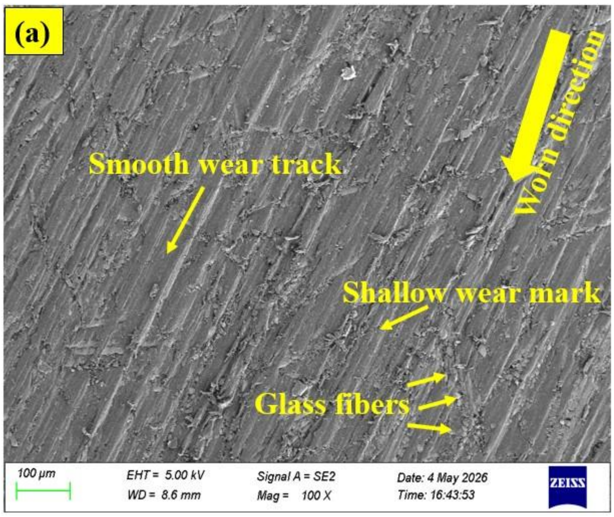

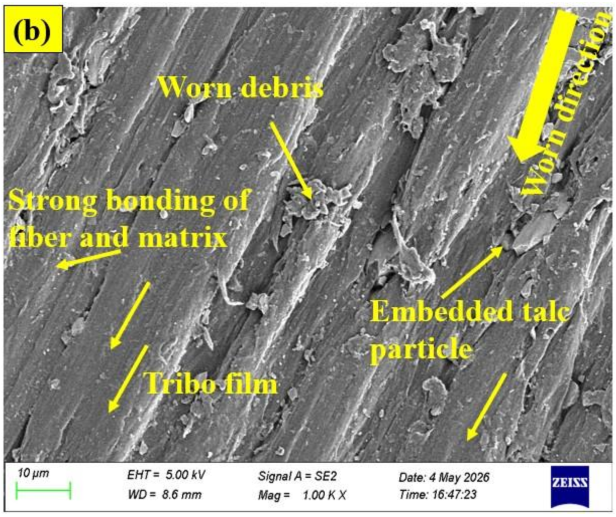

Fig. 7. Worn surface morphology of (a) PA66/SGF composite (100×) (b) PA66/SGF/T hybrid composite (1000×) abraded under a sliding distance of 75 m and applied load of 5 N.

With an increasing sliding distance (100 m) and applied load (10 N), wear of the composite transits to more complex mechanisms. Consider neat PA66, worn surface shows deep ploughing grooves and smeared regions, which is a clear sign of enhances plastic deformation and adhesive wear. Frictional heat generated during the surface interaction, soften the matrix and makes is more vulnerable to deformation and tearing. Whereas in case of PA66/SGF composite, worn morphology becomes even more heterogeneous. FESEM picture (Fig. 8a) shows partial fiber exposure and fiber-matrix de-bonding or tearing marks, results in the formation of void. Few embedded fibers begin to pullout leaving behind cavities, which further act as a stress concentrator. This lays the foundation of initiating the micro-crack formation and propagation [45]. PA66/SGF/T hybrid composite demonstrates better resistance than other PA66 composites.

Although grooves and micro-cracks are present and inevitable, the extent damage of fiber pullouts is reduced significantly which may be attributed to the improved interfacial bonding as evident from Fig. 8(b). Presence of hybrid reinforcement facilitates uniform distribution of load thereby prevents the severe damage to the maximum extent. Furthermore, at this medium wear regime, critical phenomena are observed with respect the abrasive paper effect. Also, detached glass fibers and worn debris entrapped within the abrasive paper act as third-body abrasive particle. These particles further intensify the scratching and cutting the surface which results in increasing of the grooves depth, surface roughness and wear rate.

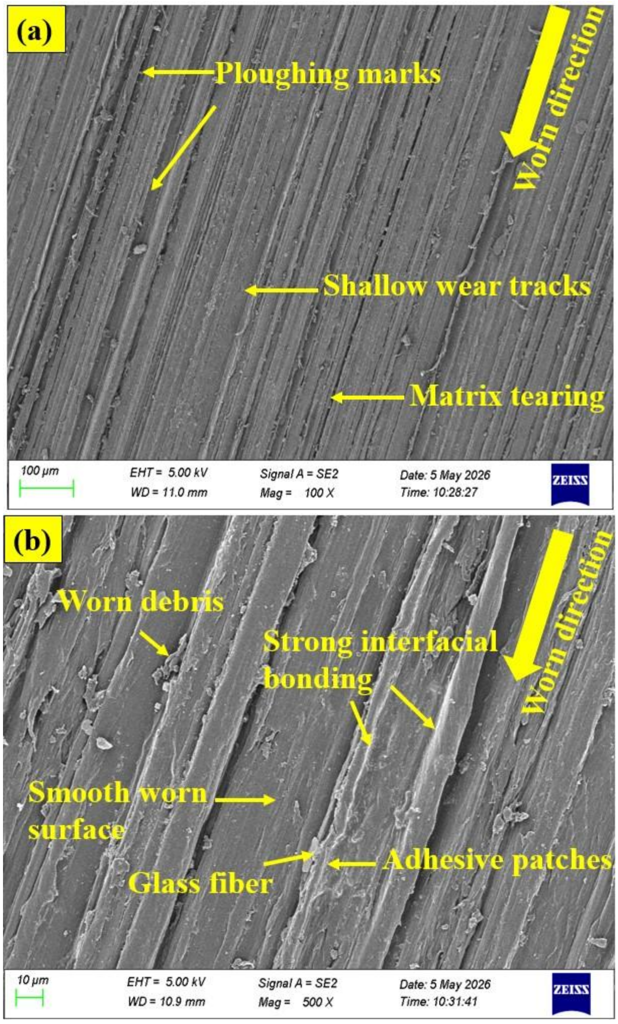

Fig. 8. Worn surface morphology of (a) PA66/SGF composite (100×) (b) PA66/SGF/T hybrid composite (500×) abraded under a sliding distance of 100 m and applied load of 10 N.

At the highest sliding distance (125 m) and applied load (15 N), wear characteristics of PA66 based composites becomes unstable and severe. Neat PA66 shows plastic deformation, smearing and tearing accompanied by the larger patches. This may be owing to the excessive frictional heating [46]. Moreover, absence of the reinforcement could be main reason for the rapid loss compared to the PA66/SGF and hybrid composites as observed in the Fig. 9(a). Abraded surface of PA66/SGF exhibits pronounced damage ascribed to fiber fracture and severe fiber pull outs. Partially broke fibers protruded from the surface act as micro-cutting tool, which further deteriorate the wear process

[44]. PA66/SGF/T hybrid composites although endured similar harsh conditions as neat PA66 and PA66/SGF, exhibits relatively better wear performance under multi-pass condition. Presence of hybrid reinforcement has been very effective in resisting crack propagation and load sharing ability. However, even this hybrid composites experienced fatigue induced fracture under intense wear condition, which is inevitable. Furthermore, at higher wear regime, accumulated broken fiber and worn debris forms the thin tribo-film at the interface, results in rapid material removal due to the aggressive cutting action as shown in Fig. 9(b).

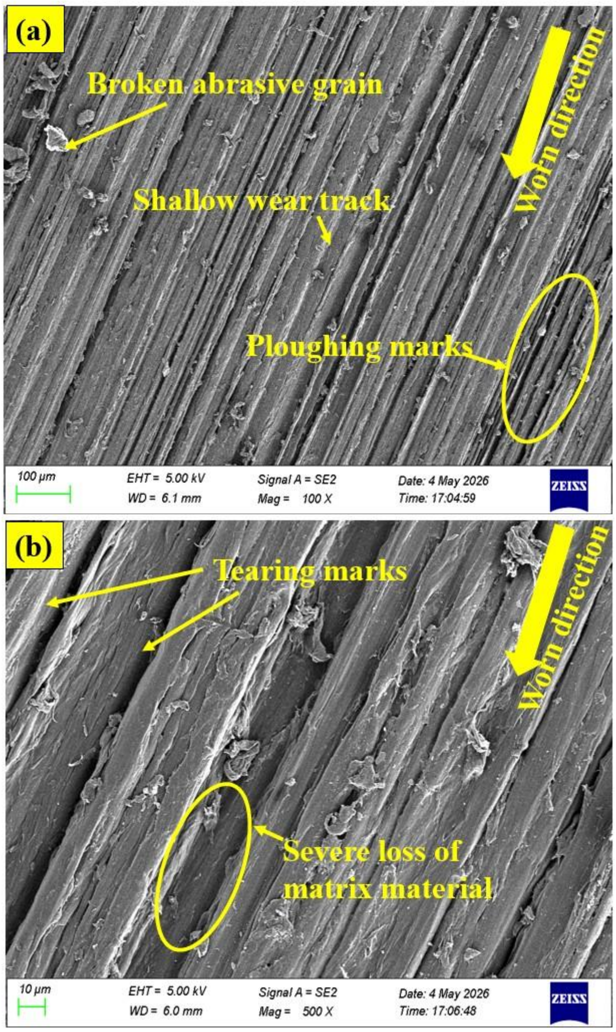

Fig. 9. Worn surface morphology of (a) PA66 (100×) (b) PA66/SGF/T hybrid composite (500×) abraded under a sliding distance of 125 m and applied load of 15 N.

Silicon carbide-based emery paper surface showed blunted abrasive grains when worn under low wear condition with an initial loss of sharp cutting edges as indicted in the Fig. 10. Although grains firmly remained embedded in the backing material, yet onset wear is evident which results in micro-cracks within in the abrasive particles. This may be attributed to the repeated sliding interaction and localized stress. Minor accumulation of the wear debris between the grains is observed however it will not hinder the abrasive surface under initial wear regime.

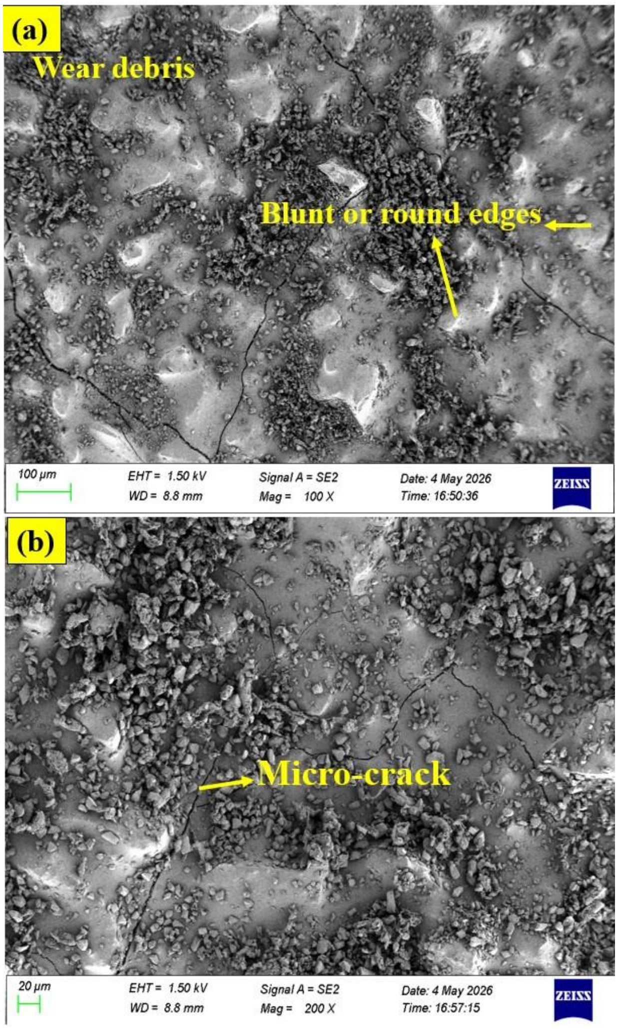

Fig. 10. Worn surface morphology of the emery paper abraded against the PA66/SGF hybrid composite at a sliding distance of 75 m and applied load 5 N under magnification 100× and 200×.

Under medium wear condition, emery paper undergoes noticeable degradation characteristics, identified as fracture of abrasive grains and broken grits as shown in the Fig. 11. Propagation of micro-cracks causes fragmentation of grains thereby produces the angular grits having secondary sharp edges. These edges increase the micro-cutting efficiency as evident from the worn surface, resulting in the fluctuation of wear behaviour. At this medium wear condition worn surface of the emery paper turns out to be heterogenous owing to the partial grain fracture and ploughings. As evident from the micrographs that, accumulation of the wear debris is significantly higher compared to the low wear regime because of which mixed wear mechanism can be observed with both cutting and ploughing including an early stage of three body abrasion ascribed to the loose fragments.

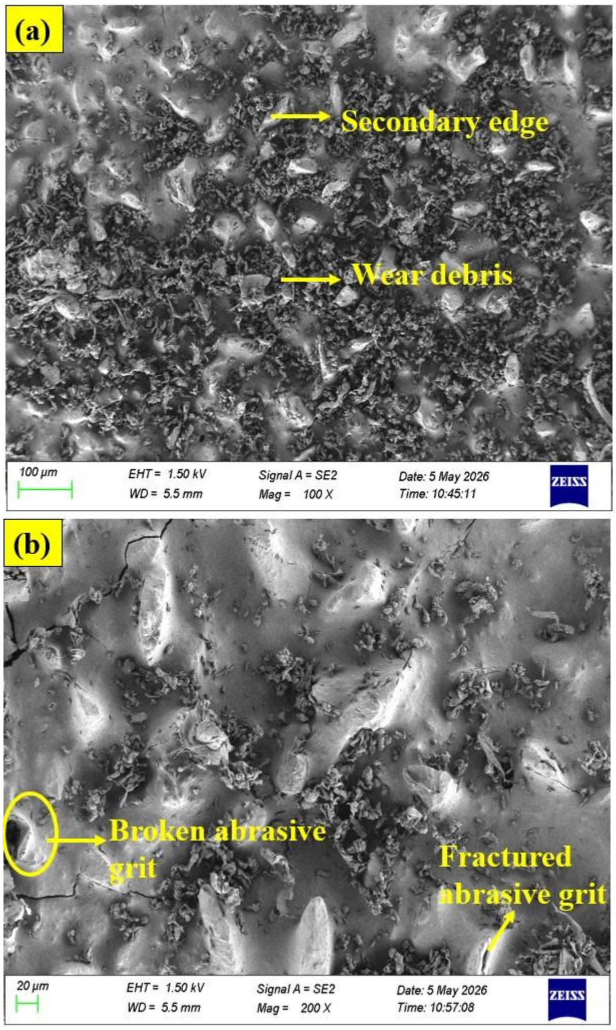

Fig. 11. Worn surface morphology of the emery paper abraded against the PA66/SGF hybrid composite at a sliding distance of 100 m and applied load 10 N under magnification 100× and 200×.

Abrasive paper severely abraded under severe wear regime, exhibiting extensive clogging and compaction of wear debris of PA66 composite as indicated in the Fig. 12. It is further evident from the micrographs that intergranular spaces are filled with polymer wear debris thereby leads to the formation of compact tribo-layer that could masks the abrasive grains. EDS spectrum (Fig. 12c) of the worn surface of the abrasive paper shows the presence of C, N and O, which is ascribed to the presence of PA66 matrix confirming the transfer of polymer material during abrasion.

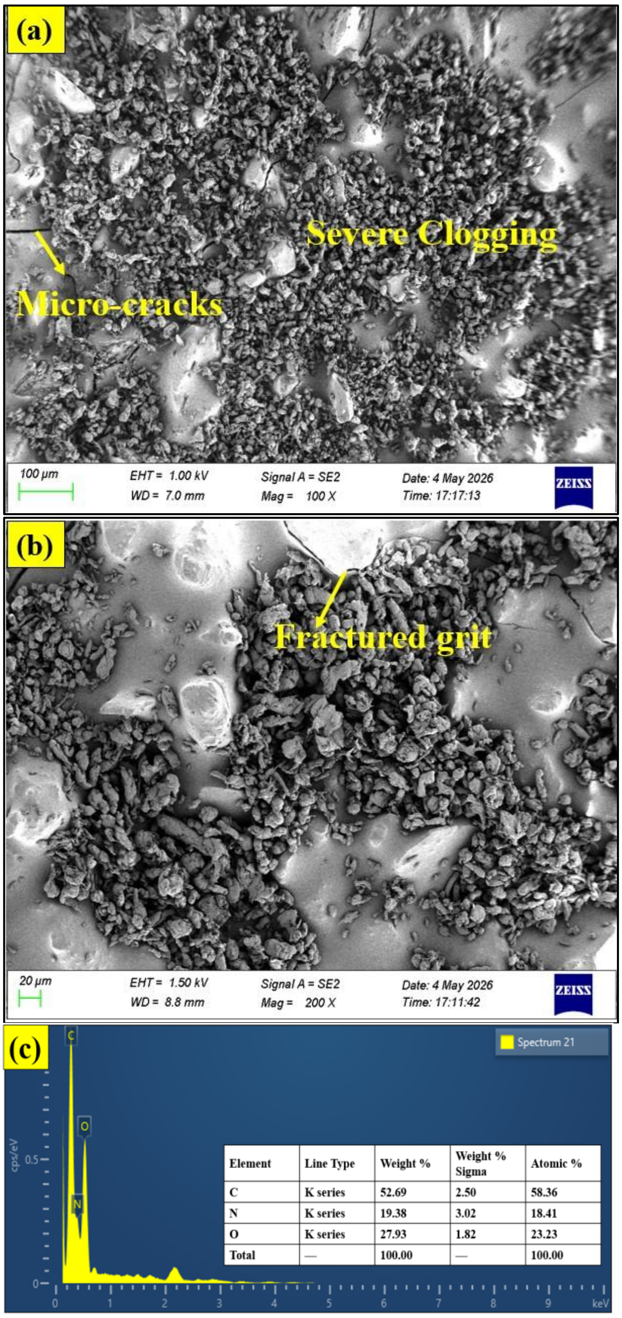

Element	Line Type	Weight %	Weight % Sigma	Atomic %
C	K series	52.69	2.50	58.36
N	K series	19.38	3.02	18.41
O	K series	27.93	1.82	23.23
Total	—	100.00	—	100.00

Fig. 12. Worn surface morphology of the emery paper abraded against the PA66/SGF hybrid composite at a sliding distance of 125 m and applied load 15 N under magnification 100× and 200×. Corresponding EDS spectrum illustrating the elemental composition of the worn surface.

However, absence of reinforcement characteristics namely, Si, Ca, or Al suggest that there may be not enough transfer of glass fiber debris onto the surface of the emery paper under the tested condition, which clearly implies that wear mechanism is predominantly influenced by matrix smearing and adhesion rather reinforcement dominated abrasion. Moreover, emery paper showed severe micro-cracking and wide spread of abrasive grit fracture as evident from the FESEM image which is clearly implies the significant loss of original grain structure. As evident that most of the abrasive particles fragmented results in less effective abrasive surface which could have been main reason for shifting of wear mechanisms from micro-cutting to ploughing, with a strong effect of three body abrasion wear owing to the loose abrasive particles. Eventually, constant accumulation of wear debris plays a vital role in deciding the overall wear performance of the PA66 based composites.

4. CONCLUSIONS

Taguchi-GRA-PCA multi-response optimization methos was employed to investigate the 2BAW performance of PA66 and its composites. The experimental results have been summarized as follows:

Experimental results revealed that specific wear rate of the PA66 composites was highly influenced by the sliding distance, reinforcement type, and applied load. SWR of the PA66 composite values found in the range 0.0210 to 0.05018 mm3/N-m, whereas COF in the range 0.020 to 0.16 and Shore D hardness value between 84 to 89. GRA transformed multiple responses such as SWR, COF and hardness into single responses. The optimal combination of input factors, A1B1C3 resulted in minimum SWR and COF with higher hardness.

ANOVA clearly showed that sliding distance (63.10%) has the highest contribution to the multi-response performance of the PA66 composites under 2BAW condition, followed by reinforcement type (7.69%) and applied load (3.94%). However, based on the p-values obtained, none of the aforementioned parameters are statistically significant at 95% confidence level. With an addition of SGF and talc filler in PA66 exhibited improved abrasion resistance property under the combination of different load and abrading distance which may be owing to strong interfacial adhesion and synergistic interaction between reinforcements.

Worn surface morphology of the PA66 composites and emery papers features debris accumulation, fiber breakages, ploughings, shallow grooves, and adhesive patches. However, major wear mechanism endured by the PA66 composites are matrix tearing, micro-ploughing and micro-cracking, clearly depends on the composite configuration, abrading distance and applied load involved.

REFERENCES

[1] Y. Şahin, A. Deniz, and F. Şahin, "Investigation of abrasive wear performances of different polyamides by response surface methodology," *Tribology in Industry*, vol. 41, no. 3, pp. 321–329, Sep. 2019, doi: 10.24874/ti.2019.41.03.02.

[2] S. Srinivas, R. Hemanth, B. Harshavardhan, G. S. Ananthapadmanabha, and B. Suresha, "Effect of surface treated nanofillers on abrasive wear of Carbon Fiber/Polyamide blend composites," *Tribology in Industry*, vol. 46, no. 4, pp. 664–676, Dec. 2024, doi: 10.24874/ti.1719.07.24.09.

[3] B. M. Rudresh and B. N. R. Kumar, "Influence of Experimental Parameters on Friction and Wear Mechanisms of PA66/PTFE Blend Reinforced with Glass Fiber," *Transactions of the Indian Institute of Metals*, vol. 71, no. 2, pp. 339–349, Jun. 2017, doi: 10.1007/s12666-017-1164-0.

[4] S. M. V. Kumar, B. Suresha, G. Rajamurugan, and A. Megalingam, "Mechanical and abrasive wear behavior of cenosphere filled carbon reinforced epoxy composites using Taguchi-Grey relational analysis," *Materials Research Express*, vol. 6, no. 1, p. 015307, Oct. 2018, doi: 10.1088/2053-1591/aae5dc.

[5] S. M. V. Kumar, E. Sakthivelmurugan, and N. Manikandaprabu, "Experimental evaluation on abrasive wear properties of Alstonia macrophylla fiber reinforced polypropylene composite using ANN model," *Proceedings of the Institution of Mechanical Engineers Part C Journal of Mechanical Engineering Science*, vol. 239, no. 15, pp. 6166–6182, Apr. 2025, doi: 10.1177/09544062251333969.

[6] P. K. Bajpai, I. Singh, and J. Madaan, "Frictional and adhesive wear performance of natural fibre reinforced polypropylene composites," *Proceedings of the Institution of Mechanical Engineers Part J Journal of Engineering Tribology*, vol. 227, no. 4, pp. 385–392, Oct. 2012, doi: 10.1177/1350650112461868.

[7] B. Briscoe, "Wear of polymers: an essay on fundamental aspects," *Tribology International*, vol. 14, no. 4, pp. 231–243, Aug. 1981, doi: 10.1016/0301-679x(81)90050-5.

[8] B. Suresha, B. N. R. Kumar, M. Venkataramareddy, and T. Jayaraju, "Role of micro/nano fillers on mechanical and tribological properties of polyamide66/polypropylene composites," *Materials & Design (1980-2015)*, vol. 31, no. 4, pp. 1993–2000, Oct. 2009, doi: 10.1016/j.matdes.2009.10.031.

[9] S. Savaş, N. Gurbanov, and M. Doğan, "Effect of fiber type, fiber content, and compatibilizer on two-body abrasive wear performance of HDPE matrix composites," *Journal of Composite Materials*, vol. 53, no. 19, pp. 2743–2760, Apr. 2019, doi: 10.1177/0021998319839135.

[10] J. Tong, Y. Ma, R. D. Arnell, and L. Ren, "Free abrasive wear behavior of UHMWPE composites filled with wollastonite fibers," *Composites Part a Applied Science and Manufacturing*, vol. 37, no. 1, pp. 38–45, Jul. 2005, doi: 10.1016/j.compositesa.2005.05.023.

[11] A. P. Harsha and U. S. Tewari, "Two-body and three-body abrasive wear behaviour of polyaryletherketone composites," *Polymer Testing*, vol. 22, no. 4, pp. 403–418, Jan. 2003, doi: 10.1016/s0142-9418(02)00121-6.

[12] B. V. Lingesh, B. N. Ravikumar, and B. M. Rudresh, "Investigation on the Effect of Grit size on Two Body Abrasive Wear Behavior of Polyamide66/Polypropylene (PA66/PP) blends," *Materials Today Proceedings*, vol. 5, no. 1, pp. 2444–2452, Jan. 2018, doi: 10.1016/j.matpr.2017.11.024.

[13] S. Zhou, Q. Zhang, C. Wu, and J. Huang, "Effect of carbon fiber reinforcement on the mechanical and tribological properties of polyamide6/polyphenylene sulfide composites," *Materials & Design* (1980-2015), vol. 44, pp. 493–499, Aug. 2012, doi: 10.1016/j.matdes.2012.08.029.

[14] B. V. Lingesh, B. N. R. Kumar, B. M. Rudresh, and H. N. Reddappa, "Effect of Micro fillers on Two Body Abrasive Wear Behavior of Polyamide 66 and Polypropylene (PA66/PP) Blend Based Composites," *Materials Today Proceedings*, vol. 5, no. 10, pp. 22376–22383, Jan. 2018, doi: 10.1016/j.matpr.2018.06.605.

[15] A. De a Lucas, J. D. Ambrósio, H. Otaguro, L. C. Costa, and J. A. M. Agnelli, "Abrasive wear of HDPE/UHMWPE blends," *Wear*, vol. 270, no. 9–10, pp. 576–583, Jan. 2011, doi: 10.1016/j.wear.2011.01.011.

[16] B. N. R. Kumar, B. Suresha, and M. Venkataramareddy, "Effect of abrasives on Three-Body abrasive wear behaviour of Particulate-Filled Polyamide66/Polypropylene nanocomposites," *Composite Interfaces*, vol. 17, no. 2–3, pp. 113–126, Jan. 2010, doi: 10.1163/092764410x490536.

[17] A. Mimaroglu, U. Sen, and H. Unal, "Abrasive wear volume maps for PA6 and PA6 composites under dry working condition," *Applied Composite Materials*, vol. 15, no. 1, pp. 13–25, Jan. 2008, doi: 10.1007/s10443-008-9054-6.

[18] S. Kumar and K. Panneerselvam, "Two-body abrasive wear behavior of Nylon 6 and glass fiber reinforced (GFR) Nylon 6 composite," *Procedia Technology*, vol. 25, pp. 1129–1136, Jan. 2016, doi: 10.1016/j.protcy.2016.08.228.

[19] B. Suresha, G. Chandramohan, N. D. Jawali, and Siddaramaiah, "Effect of short glass fiber content on Three-Body abrasive wear behaviour of polyurethane composites," *Journal of Composite Materials*, vol. 41, no. 22, pp. 2701–2713, Oct. 2007, doi: 10.1177/0021998307078730.

[20] U. S. Tewari, J. Bijwe, J. N. Mathur, and I. Sharma, "Studies on abrasive wear of carbon fibre (short) reinforced polyamide composites," *Tribology International*, vol. 25, no. 1, pp. 53–60, Jan. 1992, doi: 10.1016/0301-679x(92)90121-3.

[21] R. Senthil, V. Mohanavel, T. Raja, and M. Ali, "Tribological wear optimization of AlN strengthened with AA2024 composites through Taguchi technique," *Matéria (Rio De Janeiro)*, vol. 30, Jan. 2025, doi: 10.1590/1517-7076-rmat-2024-0839.

[22] R. Prabhu, S. Mendonca, P. K. Bellairu, R. C. DSouza, and T. Bhat, "Investigating the impact of TiO2 filler on abrasive wear characteristics of bamboo fiber-reinforced epoxy composites using the Taguchi method," *World Journal of Engineering*, vol. 22, no. 2, pp. 237–249, Jan. 2024, doi: 10.1108/wje-10-2023-0432.

[23] R. Prabhu, S. Mendonca, P. K. Bellairu, R. D'Souza, and T. Bhat, "Modeling and analysis of TiO2 filler's impact on specific wear rate in flax fiber-reinforced epoxy composite under abrasive wear using Taguchi approach," *Multidiscipline Modeling in Materials and Structures*, vol. 20, no. 3, pp. 546–557, Apr. 2024, doi: 10.1108/mmms-10-2023-0342.

[24] G. A. Kumar, J. Satheesh, K. V. S. Murthy, H. M. Mallikarjuna, N. Puneeth, and P. G. Koppad, "Optimization of wear properties of B4C Nanoparticle-Reinforced AL7075 nanocomposites using Taguchi approach," *Journal of the Institution of Engineers (India) Series D*, vol. 104, no. 1, pp. 329–340, Oct. 2022, doi: 10.1007/s40033-022-00385-3.

[25] D. Lazarevic, M. Madic, P. Jankovic, and A. Lazarevic," *Cutting parameters optimization for surface roughness in turning operation of polyethylene (PE) using Taguchi method*," Tribology in industry, vol. 34, no. 2, pp. 68, 2012.

[26] K. M. Subbaya, B. Suresha, N. Rajendra, and Y. S. Varadarajan, "Grey-based Taguchi approach for wear assessment of SiC filled carbon–epoxy composites," *Materials & Design (1980-2015)*, vol. 41, pp. 124–130, May 2012, doi: 10.1016/j.matdes.2012.04.051.

[27] M. Kamaraj, R. Manimaran, and S. Datta, "Optimization of Dry Sliding Wear Parameters of Graphene-Filled Flax Fiber-Reinforced Epoxy Composites using Taguchi Grey Relational Analysis," *Journal of the Institution of Engineers (India) Series D*, vol. 106, no. 1, pp. 85–94, Jan. 2022, doi: 10.1007/s40033-022-00331-3.

[28] M. Kumar, "Mechanical and sliding wear performance of AA356-AL2O3/SIC/Graphite alloy composite materials: Parametric and ranking optimization using Taguchi DOE and hybrid AHP-GRA method," *Silicon*, vol. 13, no. 8, pp. 2461–2477, Jul. 2020, doi: 10.1007/s12633-020-00544-9.

[29] B. P. Kumar and A. K. Birru, "Tribological Behavior of Aluminium Metal Matrix Composite with Addition of Bamboo Leaf Ash by GRA-Taguchi Method," *Tribology in Industry*, vol. 40, no. 2, pp. 311–325, Jun. 2018, doi: 10.24874/ti.2018.40.02.14.

[30] R. Rajiev, S. M. V. Kumar, H. Singh, and E. Sakthivelmurugan, "Multi-response optimization of wear parameters of flax reinforced epoxy composites using Taguchi-GRA-PCA approach," *Indian Journal of Fibre & Textile Research*, vol. 48, no. 4, Jan. 2023, doi: 10.56042/ijftr.v48i4.7640.

[31] N. J. Rathod *et al.*, "Design and optimization of process parameters for hard turning of AISI 304 stainless steel using Taguchi-GRA-PCA," *International Journal on Interactive Design and Manufacturing (IJIDeM)*, vol. 17, no. 5, pp. 2403–2414, Aug. 2022, doi: 10.1007/s12008-022-01021-w.

[32] S. Thirumalvalavan, N. Senthilkumar, G. Perumal, and M. R. A. Padmanaban, "Ameliorating the wear defiance of HVOF thermal spray Silicon carbide coated TI-6AL-4V alloy using PCA-GRA technique," *Silicon*, vol. 14, no. 6, pp. 3101–3117, Jan. 2022, doi: 10.1007/s12633-022-01706-7.

[33] Y.-L. You, D.-X. Li, G.-J. Si, R.-Y. Lv, and X. Deng, "Improvement in the tribological properties of polyamide 6," *Journal of Thermoplastic Composite Materials*, vol. 29, no. 4, pp. 494–507, Jan. 2014, doi: 10.1177/0892705713519120.

[34] N. Manikandaprabu, S. M. V. Kumar, P. Balamurugan, and B. Harshavardhan, "Enhanced erosion wear performance of TALC Particulate–Filled Glass Fiber–Reinforced Nylon66 composites: experimental analysis and machine learning based prediction," *Materials Research*, vol. 29, Jan. 2026, doi: 10.1590/1980-5373-mr-2026-0017.

[35] C. L. Morelli, A. S. Pouzada, and J. A. Sousa, "Influence of hybridization of glass fiber and talc on the mechanical performance of polypropylene composites," *Journal of Applied Polymer Science*, vol. 114, no. 6, pp. 3592–3601, Aug. 2009, doi: 10.1002/app.30980.

[36] V. K. S. Mantaiah, S. Erusagounder, R. Hemanth, S. Kannan, S. Nagulan, and R. A. Thangavel, "Experimental investigation on the mechanical behaviour of Flax/Aluminium wire mesh reinforced polypropylene hybrid composites," *Matéria (Rio De Janeiro)*, vol. 30, Jan. 2025, doi: 10.1590/1517-7076-rmat-2025-0689.

[37] S. V. Panin, V. O. Alexenko, and D. G. Buslovich, "High Performance Polymer Composites: A role of Transfer Films in Ensuring Tribological Properties—A Review," *Polymers*, vol. 14, no. 5, p. 975, Feb. 2022, doi: 10.3390/polym14050975.

[38] Y. Ren et al., "A review on tribology of polymer composite coatings," *Friction*, vol. 9, no. 3, pp. 429–470, Nov. 2020, doi: 10.1007/s40544-020-0446-4.

[39] B. N. Ramesh and B. Suresha, "Optimization of tribological parameters in abrasive wear mode of carbon-epoxy hybrid composites," *Materials & Design (1980-2015)*, vol. 59, pp. 38–49, Feb. 2014, doi: 10.1016/j.matdes.2014.02.023.

[40] H. D. S. Gowda, Hemaraju, V. G. P. Kumar, B. Suresha, C. R. Rachana, and S. K. Bhat, "Optimizing abrasive wear in sustainable MCC reinforced hemp bamboo epoxy composites for tribological applications," *Scientific Reports*, vol. 16, no. 1, Mar. 2026, doi: 10.1038/s41598-026-43505-9.

[41] H. H. Parikh, "Tribology of Plant-Based Natural Fiber Reinforced Polymer Matrix Composites – A Short review," *Journal of Natural Fibers*, vol. 20, no. 1, Feb. 2023, doi: 10.1080/15440478.2023.2172639.

[42] T. Kunishima, Y. Nagai, G. Bouvard, J.-C. Abry, V. Fridrici, and P. Kapsa, “Comparison of the tribological properties of carbon/glass fiber reinforced PA66-based composites in contact with steel, with and without grease lubrication,” *Wear*, vol. 477, p. 203899, Apr. 2021, doi: 10.1016/j.wear.2021.203899.

[43] M. M. Y. Zaghloul, K. Steel, M. Veidt, D. Martin, M. Firouzi, and M. T. Heitzmann, “Influence of Counter-Face Grit Size and Lubricant on the Abrasive Wear Behaviour of Thermoplastic Polymers Reinforced with Glass Fibres,” *Tribology Letters*, vol. 71, no. 3, Aug. 2023, doi: 10.1007/s11249-023-01774-9.

[44] R. Autay, S. Missaoui, J. Mars, and F. Dammak, “Mechanical and tribological study of short glass fiber-reinforced PA 66,” *Polymers and Polymer Composites*, vol. 27, no. 9, pp. 587–596, Jun. 2019, doi: 10.1177/0967391119853956.

[45] T. B. Yallew, P. Kumar, and I. Singh, “Sliding behaviour of woven industrial hemp fabric reinforced thermoplastic polymer composites,” *International Journal of Plastics Technology*, vol. 19, no. 2, pp. 347–362, Dec. 2015, doi: 10.1007/s12588-015-9121-4.

[46] K. K. Basumatary, N. Mohanta, and S. K. Acharya, “Effect of fiber loading on abrasive wear behaviour of Ipomoea carnea reinforced epoxy composite,” *International Journal of Plastics Technology*, vol. 18, no. 1, pp. 64–74, May 2014, doi: 10.1007/s12588-014-9065-0.